

## Analysis of Counter-Current Interaction Between Matrix and Fracture for Gas-Water Systems

Tayfun Babadagli and Can Ulas Hatiboglu

University of Alberta, Dept. of Civil and Environmental Eng., School of Mining and Petroleum

[tayfun@ualberta.ca](mailto:tayfun@ualberta.ca) and [canh@ualberta.ca](mailto:canh@ualberta.ca)

**Keywords:** Counter-current, capillary imbibition, matrix shape factor, residual gas saturation, gas recovery rate, high temperature, sandstone, limestone.

### ABSTRACT

Counter current matrix-fracture interaction is a commonly encountered process in production of geothermal fluids. In this paper we address different aspects of this phenomenon.

The rate of imbibition transfer and the development of residual gas phase under low (20°C) and high temperatures (90 °C) were examined experimentally. Cylindrical Berea sandstone and Indiana limestone samples with different shape factors were obtained by cutting the plugs 1, 2.5, and 5 cm in diameter and 2.5, 5, and 10 cm in length. All sides were coated with epoxy except one end. Static imbibition experiments were conducted on vertically and laterally situated samples where the matrix-fracture interaction took place upward and lateral (horizontal) directions, respectively. Brine and air were used as wetting and non-wetting phases, respectively.

The experimental scheme followed was useful in identification of the development of residual gas saturation for fully counter-current matrix-fracture interaction. We investigated and clarified to what degrees the rock/fluid properties (wettability and matrix shape factor) and existing conditions (temperature, causing lowered surface tension and brine viscosity, and gravity) become effective on the residual gas saturation. Finally, critical matrix and fluid properties were correlated to the residual gas saturation and recovery rate.

### 1. INTRODUCTION

Gas phase in the matrix of naturally fractured gas and geothermal reservoirs can be produced if there exists a liquid phase in fractures by capillary or gravity interaction. Mechanism is counter-current, i.e., displacement of non-wetting phase by wetting phase takes place from the same side of the matrix, if the boundary conditions physically restricting the contact of wetting phase with matrix from the other sides exist. Understanding the dynamics of counter-current imbibition is crucial to cure recovery problems in gas and geothermal reservoirs. It has recently been observed that the residual non-wetting phase saturation in gas-liquid systems is highly dependent on the boundary condition if the interaction is counter-current (Hatiboglu and Babadagli, 2004). Although the mobility ratio and wettability are more favorable in gas-liquid systems, high surface tension may cause the entrapment of non-wetting phase gas phase. This is more prominent in case of counter-current flow as the boundary effects also play a significant role in the development of residual non-wetting phase compared to the liquid-liquid interactions.

Development of gas (non-wetting phase) saturation at ambient conditions has been investigated in the past for

spontaneous (capillary) imbibition (Kantzias et al., 1997; Pow et al., 1999; Kantzas et al., 2001; Li and Horne, 2001; Hamon, et al., 2001; Ding and Kantzas, 2002; Egermann et al., 2004). Some of these studies dealt with counter-current imbibition. Counter-current imbibition of liquid-liquid systems was studies in comparison to the other types of interactions (Bourbiaux and Kalaydjian, 1988; Zhang et al., 1996; Zhou et al., 2001; Babadagli, 2001 and 2002). It is highly expected that the capillary imbibition of gas-liquid systems differs from that of liquid-liquid systems, especially for counter-current imbibition. Therefore, detailed analyses for the effects of the boundary conditions restricting the interaction between matrix and fracture and causing a counter-current imbibition are still needed. The boundary conditions (can also be described as the matrix shape factor) can be a critical parameter on the residual non-wetting phase saturation in case of counter-current imbibition. Zhou et al. (2001) discussed this for oil-water systems. They observed that the residual oil distribution is more sensitive to local heterogeneity in case of counter-current imbibition and a frontal displacement of air by water in diatomite samples is obtained due to capillary imbibition. They also reported that the counter-current imbibition initially yields a higher recovery rate than co-current but the residual oil saturation is 20% less than that of co-current. Hatiboglu and Babadagli (2004) observed that the residual non-wetting phase in gas-oil systems is more sensitive to the boundary conditions compared to the liquid-liquid systems.

The recovery rate and ultimate recovery in naturally fractured gas and geothermal reservoirs are mainly controlled by the interaction type. Matrix shape, i.e., boundary conditions, is one of the critical parameters that is not controllable. Therefore, controllable parameters such as the viscosity of injected fluid, surface tension, temperature etc. could be adjusted based on the matrix characteristics for efficient matrix fracture interaction. Although the capillary imbibition from a matrix with all sides open to flow has been investigated extensively, understanding the dynamics of counter-current imbibition needs more research. Especially, in deriving the relative permeability correlations for counter-current flow, the end point values, i.e., the residual saturations, are the most critical parameters to be measured. Rock and fluid properties playing a role in the capillary imbibition has been studies after pioneering work by Mattax and Kyte (1962). Recently, Morrow and Mason (2001) reviewed the studies published on capillary imbibition of liquid-liquid systems in the last four decades. It is agreed that the gas-liquid systems may differ from liquid-liquid systems and the approaches used to describe and formulate the phenomenon, i.e., the scaling groups, may not be applicable for gas-liquid systems mainly due to the differences in density, viscosity, surface tension, and wettabilities of the phases.

Further investigation is also needed to clarify the effects of higher temperatures on the capillary imbibition of gas-liquid systems. As mentioned earlier, the residual oil

development is more severe in counter-current imbibition of gas-liquid systems. Higher temperature experiments would both help understand the effect of temperature on the residual non-wetting phase and clarify the causes of the gas entrapment by changing the surface tension and viscosity but not boundary conditions.

The objective of this paper is to understand the dynamics of the counter-current displacement of non-wetting (gas) phase by a wetting phase (water) due to capillary forces at different temperatures. It is also aimed to identify the effect of matrix shape factor and interfacial forces that are subject to change with increasing temperature on the rate and ultimate recovery.

## 2. EXPERIMENTAL STUDY

### 2.1 Materials

Cores used were Berea sandstone ( $\phi=21\%$  and  $k=500$  mD) and Indiana limestone ( $\phi=16\%$  and  $k=15$  mD) samples with 3 different diameters:  $\frac{1}{2}$ , 1, and 2 inches. Each diameter was available in 3 different lengths: 2, 4 and 6 inches (Fig. 1). The samples were coated with epoxy, leaving only one side open to imbibition. Table 1 lists the core specifications and orientations for different experiments. Fig. 1 displays the shapes and dimensions of the cores used in the experiments. The properties of the fluids used and surface tensions are given in Table 2.

### 2.1 Procedure

After cutting and coating the cores, air-water imbibition experiments were performed using the imbibition tubes. Vertically and horizontally positioned cores were exposed to the wetting-phase. Small and large imbibition tubes were utilized for large and small core experiments. The tubes are made of glass, with a graduated cylinder on top to monitor the volume imbibed. The small imbibition tubes are of 2 inches in diameter and 4 inches in length. The graduated cylinder attached has a volume of 12cc, with a 0.1cc scale. The large tube is 70mm in diameter and 7 inches in length. These tubes also have off-set positioned graduated cylinders to be able to monitor the recovery for the horizontal imbibition experiments. The volume of the graduated cylinder is 50cc to accommodate the large volumes of recoveries. Small graduated cylinders may be attached to these tubes via elastic tubing to ensure precise readings. For high temperature experiments, the imbibition tubes were placed in a temperature bath using a hanging line that was attached to a scale. Before doing this, the rock sample and water were preheated to 90°C. Water used in the experiments was deaerated to avoid any gas phase coming out of it at higher temperatures. The amount of water imbibition was monitored by reading the change in the scale. Note that the vertically positioned cores have the open surface pointing downwards to allow wetting phase imbibition only against the gravity.

## 2. ANALYSIS OF THE RESULTS

### 2.1 Experiments at 20°C

Air-water imbibition recovery curves for the Berea sandstone experiments at the ambient conditions are shown in Figs. 2 and 3. They include all different combinations of diameter, length, and orientation given in Table 1. Small diameter cores (Exps. 1, 2, and 3) yielded the most efficient displacement for the vertical cases (Fig. 2). They all showed a similar recovery rate and ultimate recovery regardless the aspect ratio. In other words, the matrix

boundary conditions were not observed to be effective for the small diameter samples.

The 1 and 2" diameter cores, however, resulted in a lower displacement efficiency, which is a sign of a bullet profiled water front. Boundary effects are significant especially for long (6 inches) cores. A hump in the middle of the curve is an indication of the water front reaching the no-flow boundary (see, for example, the curve Exp. 6 in Fig. 2). The imbibition continues laterally afterwards with a lower rate. The rate of imbibition was highly affected by the increasing diameter (or diameter/length ratio) of the core.

One uncoated case of vertically situated sample (Exp. 25) was included in this analysis for comparison. Exps. 25 and 4 are the same size cores with different boundary conditions. Although the recovery rates did not show a significant difference (it is even faster for the counter-current imbibition at early times), 16% higher recovery was obtained from the uncoated sample. Note that all small diameter samples yielded a faster recovery than the uncoated sample. A remarkable difference in the ultimate recoveries was also obtained between the smallest diameter samples (blue lines in Fig. 2) and Exp. 25. Due to the size of the sample (the longest and the largest diameter) and the difference in the densities of the phases, it is expected that the gravity effect is not negligible even if the all sides of matrix is open to flow. The hump in the middle of the curve can be attributed to the transition from the capillary imbibition (likely to be in counter-current manner due to strong water wettability) to the gravity dominated flow (due to significant different in the density difference).

Horizontally positioned cores resulted in slightly higher ultimate recovery values than that of vertical ones as expected (Fig. 3). The boundary effect is more significant. The smallest diameter samples showed a similar behavior to the cases of vertically situated samples except the shortest one (Exp. 10). A hump caused by the front reaching the no-flow end of the core is more prominent in the horizontal cases (see Exps. 16 and 17).

One uncoated case (Exp. 26) was also included in this analysis for comparison. Exps. 26 and 18 are the same size cores with different boundary conditions. Obviously, the uncoated core yielded much faster recovery than not only the same size of cores but also all the other samples. The difference in the ultimate recovery is 16 % between Exp. 26 and Exp. 18. Note that the two smallest diameter samples (Exps. 11 and 12) yielded slower recovery rate but higher ultimate recovery than the uncoated samples despite the counter-current interaction type, as similar to the vertical cases shown in Fig. 2.

### 2.1 Experiments at 90°C

Air-water imbibition recovery curves for Berea sandstone experiments at higher temperature (90°C) conditions are shown in Figs. 4 and 5. They include all different combinations of diameter, length, and orientation given in Table 1. Both vertical and horizontal cases showed different behavior at elevated temperatures compared to the experiments conducted at 20°C. The improvement in the recovery rate was obtained for all the samples at elevated temperature and this can be attributed to the threefold lowered viscosity of water (Table 2). The faster recovery is more notable for shorter samples. Humps on the curves were observed for higher length/diameter samples, i.e., Exps. H-3 and H-6. Note that these humps were observed for all 1 and 2" diameter cases of low temperature vertical experiments (Fig. 2). An interesting point is the low recovery with the smallest sample (Exp. H-1) for the vertical case. When compared to the low temperature case

(Exp. 1 in Fig. 2), remarkable difference in the recovery rate is prominent (13%).

The horizontal experiments showed a typical trend: Smaller the length, faster the recovery for any given diameter. A significant improvement in ultimate recovery was obtained with increasing temperature especially for 2" diameter samples. The uncoated sample (Exp. H-26) recovered the same amount of oil as the coated sample (Exp. H-1) of the same dimensions even though the latter yielded much slower recovery. This could be attributed to the reduced surface tension with temperature (Table 2).

## 2.1 Residual gas saturation

It is also intended to understand the development of residual gas saturation depending on the matrix shape factor and temperature in this study. For low temperature experiments, as the core gets more elongated, a decrease in the residual gas saturation is observed. This is more prominent in the larger diameter cores for vertical flow. The effect of the diameter of the core on the residual oil is more significant in the horizontal case. The increased temperature not necessarily yielded a higher ultimate recover. Although all the cases of horizontal samples showed an improvement in the ultimate recovery, only 1-inch diameter samples resulted in an increase in the ultimate recovery for vertical cases.

Different attempts were made to correlate the residual gas saturation to different rock and fluid characteristics such as the matrix shape factor, length to diameter ratio etc. A trend was obtained for vertical and horizontal cases at high and low temperatures, respectively when a newly defined dimensionless group (see Eq. 5 below) was used.

Mattax and Kyte (1962) demonstrated that the imbibition recovery of oil could be scaled by plotting normalized recovery against the dimensionless time, defined as:

$$t_D = \left( \sqrt{\frac{k}{\phi \mu_w}} \frac{\sigma}{L^2} \right) t \quad (1)$$

The modified form of this equation was proposed later as follows (Zhang et al., 1996):

$$t_D = 0.02 \left( \sqrt{\frac{k}{\phi \mu_{gm}}} \frac{\sigma}{L_c^2} \right) t \quad (2)$$

where  $t_D$  is dimensionless time,  $k$  permeability in md,  $\phi$  fractional porosity,  $\sigma$  interfacial tension in dynes/cm,  $L_c$  characteristic length in cm, and  $t$  time in minutes. The term  $\mu_{gm}$  represents geometric mean viscosity in cp, which, for an oil/water system, is given by:

$$\mu_{gm} = \sqrt{\mu_o \mu_w} \quad (3)$$

$L_c$ , the characteristic length is defined as follows (Zhang et al., 1996):

$$L_c = \sqrt{\frac{V}{\sum_{i=1}^n \frac{A_i}{X_{Ai}}}} \quad (4)$$

where  $V$  is the bulk volume of the matrix,  $A_i$  is the area open to imbibition at the  $i^{\text{th}}$  direction, and  $X_{Ai}$  is the distance

traveled by the imbibition front from the open surface to the no-flow boundary.

We propose the following dimensionless group to be correlated to the residual gas phase saturation:

$$t_D = 0.02 \left( \sqrt{\frac{k}{\phi \mu_{gm}}} \frac{\sigma}{L_c^2} \right) t_{final} \quad (5)$$

For the time value in Eq. 2, the time that the imbibition reaches plateau region, i.e., the point where the ultimate recovery is reached, was used in Eq. 5 ( $t_{final}$ ). This dimensionless group, in a sense, represents the efficiency of the process as it considers both the time needed to reach the ultimate recovery and the final recovery.

Figs. 6 and 7 display the change of residual gas saturation with the dimensionless group defined in Eq. 5 for low and high temperatures, respectively. Decreasing residual gas saturation was obtained with the  $t_D$  for both cases. In these plots the residual gas saturations obtained for Indianan limestone samples (Table 1) were also included. For the higher temperature cases, a trend was obtained only for the vertical cases (Fig. 7). In fact, there exist two different trends as indicated by the solid and dashed lines. Most of the experiments fell onto the trend shown by a dashed line except three experiments. Those three cases (H-8, H-20, and H-21) yielded high residual gas phase saturation and they are the largest samples (Table 1).

## 3. DISCUSSION

Counter-current imbibition of air and water was studied experimentally for different matrix shape factors at different temperatures. Main purpose was to investigate the dynamics of spontaneous imbibition displacement in conjunction with the development of residual gas.

Air-water imbibition plots show high sensitivity to orientation as the gravity dominates when the cores are positioned vertically. Despite the favorable wettability and viscosity values, the air-water imbibition may take long time to fully imbibe depending on the shape of the core. Smaller cores with small diameter yield faster imbibition rates with higher ultimate recovery. A hump was observed for large and long cores, which is an indication of the bullet shaped water front. After reaching the no-flow boundary, that was indicated by the hump, slower displacement was observed. Horizontal and vertical orientations did not show much difference in the ultimate recovery.

For the low temperature experiments, residual gas saturations for air-water systems display an increasing trend with respect to dimensionless group (Eq. 5). A decreasing trend with respect to the elongation factor (Length/Diameter) of the cores, which is a sign of bullet shaped displacement profile, was also observed for the small diameter cores. Typically, Length/Diameter = 4 was found to be a threshold value at which the most efficient recovery was obtained. This is an indication of the existence of an optimal core diameter or diameter to length ratio.

Although the horizontal cases did not show any significant change in terms of the recovery -rate- trend (but showed an increase in the ultimate recovery), the vertical cases yielded different recovery rates and ultimate recoveries at elevated temperature (90°C). Reduced gas saturation was obtained only for certain core sizes (typically high diameters) with increasing temperature. That was attributed to the reduction in surface tension.

There are some other factors that might affect the imbibition recovery but were not investigated in this study. One of them is the initial water. Significant effects of initial water on the recovery rate and ultimate recovery was observed on the samples open to flow from all sides by Li and Horne (2002). Also, the gravity effect has not been included in the correlations between the dimensionless group and the residual gas saturation. This part of the study is on-going. The changes in the recovery behavior at higher temperature were mainly attributed to slight reduction in surface tension and water viscosity.

No phase change is expected at the given temperature range. The changes in the liquid phase existing in the rock can be an additional driving force to enhance the displacement of the gas phase (Udel, 1985; Birkholzer, 2003) at higher temperatures. The change in the property of the liquid imbibition into the rock is expected to be minimal as well as the expansion of gas phase in the rock (the rock was pre-heated to the temperature) at the given temperature range. The capillary interaction was mainly controlled by the core dimensions (or the shape factor) and the change in the surface tension and viscosity of the phases at higher temperature. Further investigation will also be on this area as well as the effect of temperature gradient on the capillary imbibition (Medina et al, 2003) as the higher temperatures are expected in geothermal reservoir matrix.

## CONCLUSIONS

1. The effects of matrix boundary conditions, yielding only counter-current interaction, on the recovery rate and the ultimate recovery were identified for different temperatures experimentally. Wide ranges of matrix length/diameter ratios, i.e., shape factor, were applied.
2. Optimum core size in air-water case was observed to be 0.5 inch diameter and 6 inches of length, both in terms of the recovery rate and ultimate recovery for low temperature experiments.
3. Residual gas saturation is sensitive to the matrix shape factor (or core dimensions) for the counter-current imbibition of water into gas saturated systems.
4. The effect of surface tension on the recovery rate and ultimate recovery in the counter-current type interaction is critical. Although the horizontal cases did not show any significant change in terms of the recovery trend (but showed an increase in the ultimate recovery), the vertical cases yielded different recovery rates and ultimate recoveries with increasing temperature. Lower residual gas saturation was obtained only for certain core sizes (typically high diameters) with increasing temperature. That was attributed to the reduction in surface tension.

## ACKNOWLEDGEMENTS

This study was funded in part by an NSERC Grant (No: G121210595). The authors gratefully acknowledge this support. The authors also wish to thank Mr. Sean Watt for the assistance during the experimental work.

## REFERENCES

Babadagli, T.: Dynamics of Capillary Imbibition When Surfactant, Polymer, and Hot Water Are Used as Aqueous Phase for Oil Recovery, *J. Coll. and Int. Sci.*, vol. 246, 2002, 203.

Babadagli, T.: Scaling of Cocurrent and Countercurrent Capillary Imbibition for Surfactant and Polymer Injection in Naturally Fractured Reservoirs, *SPE Journal* (Dec. 2001) 465-478.

Birholzer, J.: Penetration of Liquid Fingers into Superheated Fractured Rock, *Water Res. Res.* Vol. 39, no. 4, 2003, SBH 9.

Bourbiaux, B. J. and Kalaydjian, F. J.: Experimental Study of Cocurrent and Countercurrent Flows in Natural Porous Media, paper SPE 18283, presented at the 1988 SPE Annual Tech. Conf. and Exh., Houston, Oct. 2-5.

Ding, M. and Kantzas, A.: Residual Gas Saturation Investigation of a carbonate Reservoir from Western Canada, SPE 75722 presented at the 2002 SPE Gas Tech. Symp., Calgary, Canada, 30 April – 2 May.

Egerman, P., Laroche, C., Manceau, E., Delamaide, E. and Bourbiaux, B.: Experimental and Numerical Study of Water-Gas Imbibition Phenomena in Vuggy Carbonates, SPE 89421 presented at the 2004 SPE/DOE 14<sup>th</sup> Symp. on Imp. Oil Rec., Tulsa, OK, 17-21 April.

Hamon, G., Suzanne, K., Billiotte, J. and Trocme, V.: Field-Wide Variations of Trapped Gas Saturation in Heterogeneous Sandstone Reservoirs, SPE 71524 presented at the 2001 SPE Annual Tech. Conf. And Exh., New Orleans, LA, 30 Sept. – 3 Oct.

Hatiboglu, C. U. and Babadagli, T.: Dynamics Of Spontaneous Counter-Current Imbibition For Different Matrix Shape Factors, Interfacial Tensions, Wettabilities and Oil Types, Paper 2004-091, CIM 55<sup>th</sup> Annual Technical Meeting, Canadian International Petroleum Conference, Calgary, Canada, 8-10 June 2004.

Kantzas, A., Pow, M. Allsopp, K. and Marenette, D.: Co-current and Counter-current Imbibition Analysis for Tight Fractured Carbonate Gas Reservoirs, paper 97-181, presented at the 7<sup>th</sup> Pet. Soc. of CIM Petroleum Conf. of the South Saskatchewan Section, 1997.

Kantzas, A., Ding, M., and Lee, J.: "Residual Gas Saturation Revisited," *SPE Res. Eval. & Eng.*, vol. 4, no. 6, Dec., 2001, 467.

Li, K. and Horne, R.N.: "Characterization of Spontaneous Water Imbibition into Gas-Saturated Rocks, *SPEJ*, Dec., 2001, 375.

Li, K. and Horne, R.N.: "Scaling of Spontaneous Imbibition in Gas-Liquid Systems, SPE 75167 presented at the 2002 SPE/DOE Imp. Oil Rec. Symp., Tulsa, OK, 13-17 April.

Mattax, C. C. and Kyte J. R.: "Imbibition Oil Recovery from Fractured, Water-Drive Reservoir, *SPEJ*, June, 1962, 177.

Medina, A., Pineda, A. and Trevino, C.: Imbibition Driven by a Temperature Gradient, *J. of the Physical Soc. Of Japan*, Vol. 72, no. 5, 2003, 979.

Morrow, N.R. and Mason, G.: Recovery of Oil by Spontaneous Imbibition, *Current Opinion in Coll.&Int. Sci.* Vol. 6, 2001, 321.

Pow, M., Kantzas, A., Allan, V. and Mallmes, R.: "Production of Gas from Tight Naturally Fractured Reservoirs with Active Drive, *JCPT*, vol. 38, no. 7, July, 199, 38.

Udell, K.S.: Heat Transfer in Porous Media Considering Phase Change and Capillarity – The Heat Pipe Effect,

*Int. J. Heat and Mass Transfer.* Vol. 28, no. 2, 1985, 485.

Zhang, X., Morrow, N. R., and Ma, S.: Experimental Verification of a Modified Scaling Group for Spontaneous Imbibition, *SPERE*, Nov. 1996, 280.

Zhou, D., Jia, L., Kamath, J., and Kovscek, A.R.: An Investigation of Counter-Current Imbibition Process in Diatomite, SPE 68837 presented at the 2001 SPE Western Reg. Meet., Bakersfield, CA, 26-30 March.

**Table 1: Experiments conducted throughout the study.**

| CORE SIZES and POSITIONS |               |          | EXPERIMENTS @ T = 20°C |                   |                        | EXPERIMENTS @ T = 90°C |                   |                        |
|--------------------------|---------------|----------|------------------------|-------------------|------------------------|------------------------|-------------------|------------------------|
| Length (in)              | Diameter (in) | Position | Berea Sandstone        | Indiana Limestone | Uncoated (Berea Sand.) | Berea Sandstone        | Indiana Limestone | Uncoated (Berea Sand.) |
| 2                        | 0.5           | Ver.     | 1                      |                   |                        | H-1                    |                   |                        |
| 4                        | 0.5           | Ver.     | 2                      |                   |                        | H-2                    |                   |                        |
| 6                        | 0.5           | Ver.     | 3                      |                   |                        | H-3                    |                   |                        |
| 2                        | 1             | Ver.     | 4                      |                   | 25                     | H-4                    |                   | H-25                   |
| 4                        | 1             | Ver.     | 5                      |                   |                        | H-5                    |                   |                        |
| 6                        | 1             | Ver.     | 6                      |                   |                        | H-6                    |                   |                        |
| 2                        | 2             | Ver.     | 7                      | 19                |                        | H-7                    | H-19              |                        |
| 4                        | 2             | Ver.     | 8                      | 20                |                        | H-8                    | H-20              |                        |
| 6                        | 2             | Ver.     | 9                      | 21                |                        | H-9                    | H-21              |                        |
| 2                        | 0.5           | Hor.     | 10                     |                   |                        | H-10                   |                   |                        |
| 4                        | 0.5           | Hor.     | 11                     |                   |                        | H-11                   |                   |                        |
| 6                        | 0.5           | Hor.     | 12                     |                   |                        | H-12                   |                   |                        |
| 2                        | 1             | Hor.     | 13                     |                   |                        | H-13                   |                   |                        |
| 4                        | 1             | Hor.     | 14                     |                   |                        | H-14                   |                   |                        |
| 6                        | 1             | Hor.     | 15                     |                   |                        | H-15                   |                   |                        |
| 2                        | 2             | Hor.     | 16                     | 22                |                        | H-16                   | H-22              |                        |
| 4                        | 2             | Hor.     | 17                     | 23                |                        | H-17                   | H-23              |                        |
| 6                        | 2             | Hor.     | 18                     | 24                | 26                     | H-18                   | H-24              | H-26                   |

Ver.: Vertical, Hor.: Horizontal

**Table 2: Properties of the fluids used in the experiments.**

|                           | Wetting Phase   |                  | Non-Wetting Phase |
|---------------------------|-----------------|------------------|-------------------|
|                           | Hot Water (90°) | Cold Water (25°) | Air               |
| Density (g/cc)            | 0.965           | 1                | 0.001             |
| Viscosity (cp)            | 0.326           | 1                | 0.182             |
| Surface Tension (dyne/cm) | 60.8            | 72.9             |                   |

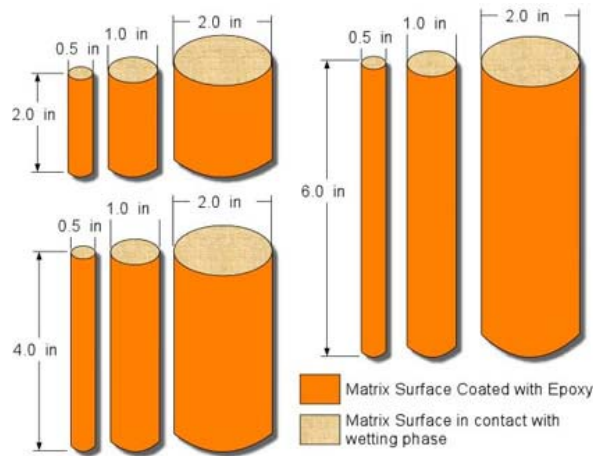


Figure 1: The sizes and shapes of the cores used in the experiments.

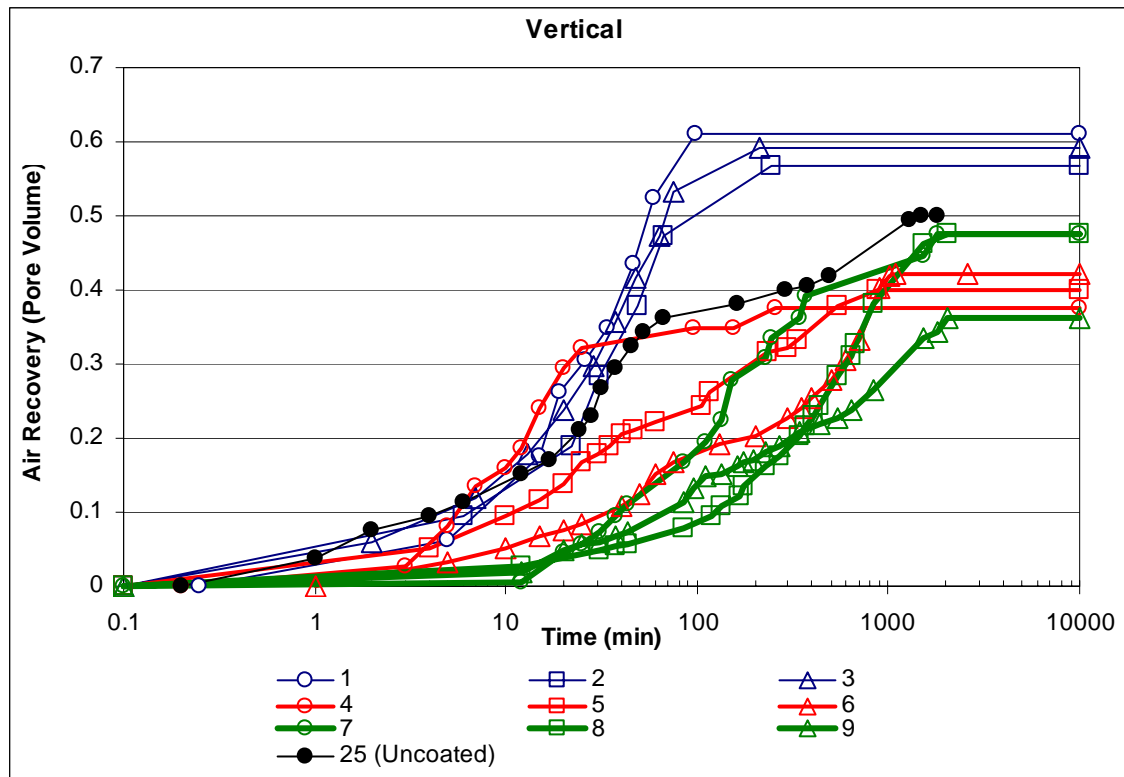


Figure 2: Air recovery by capillary imbibition of water from different matrix sizes and shapes for vertically positioned samples at  $T=20^{\circ}\text{C}$ .

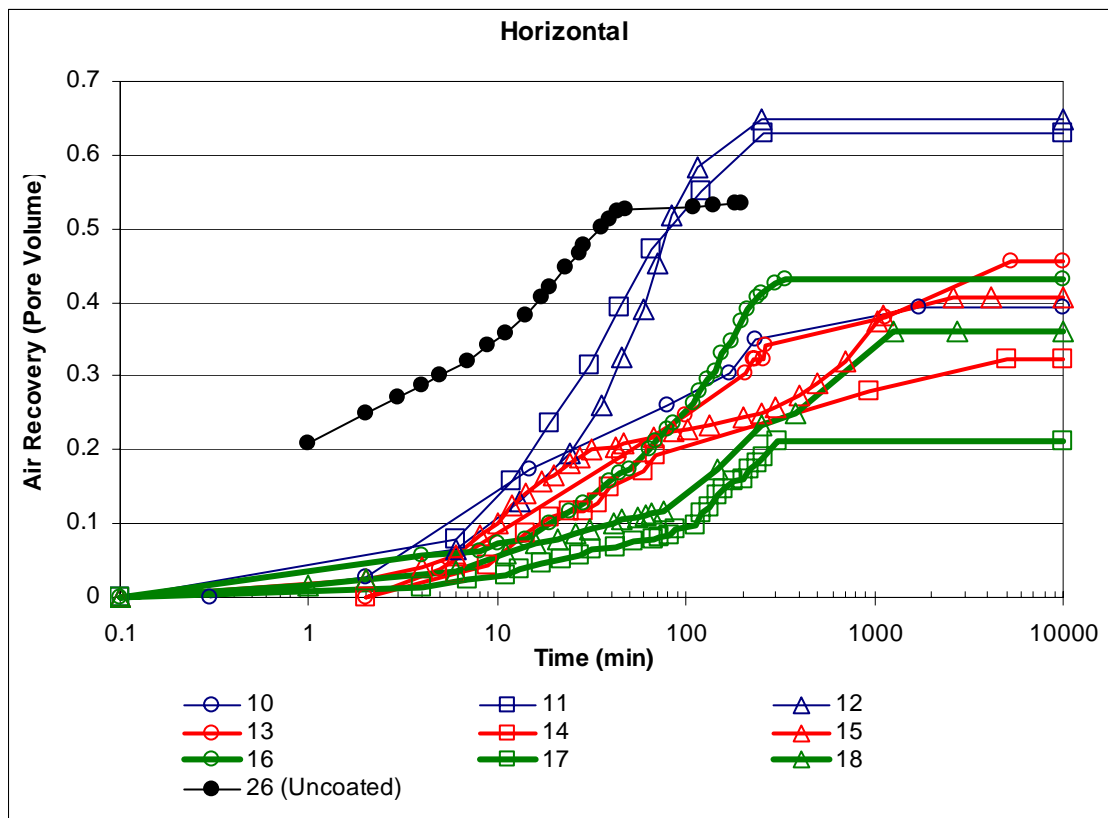


Figure 3: Air recovery by capillary imbibition of water from different matrix sizes and shapes for horizontally positioned samples at  $T=20^{\circ}\text{C}$ .

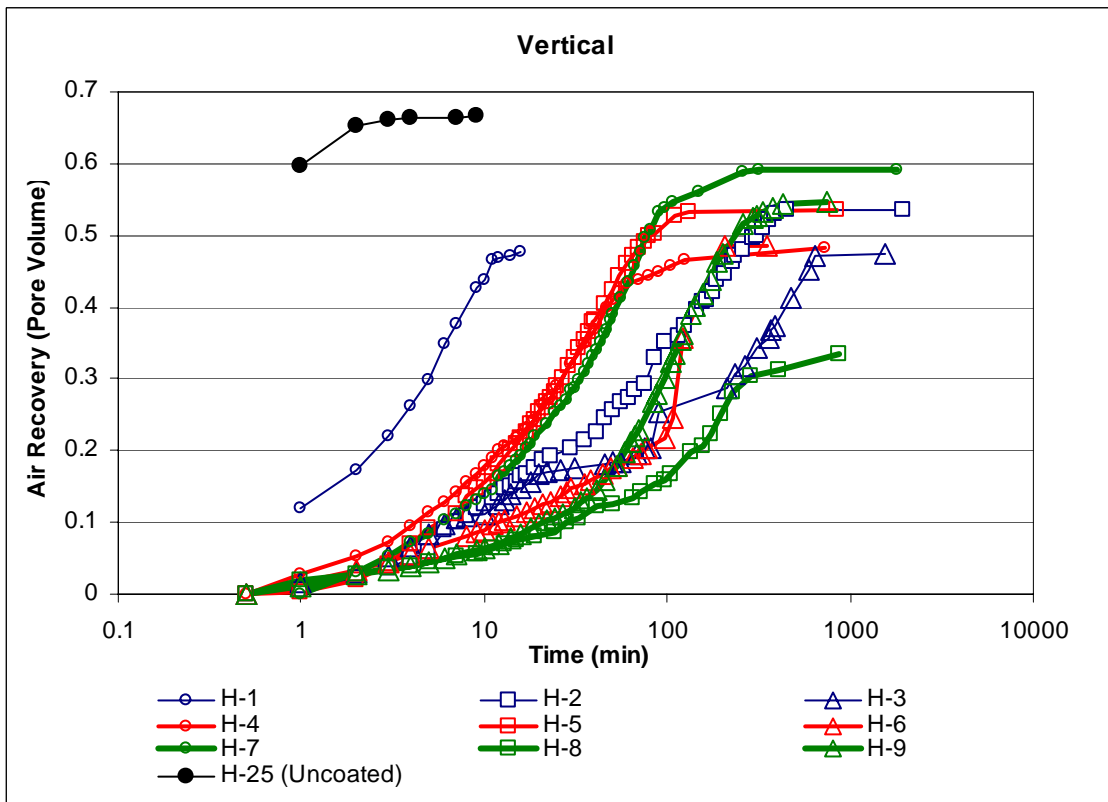


Figure 4: Air recovery by capillary imbibition of water from different matrix sizes and shapes for vertically positioned samples at  $T=90^{\circ}\text{C}$ .

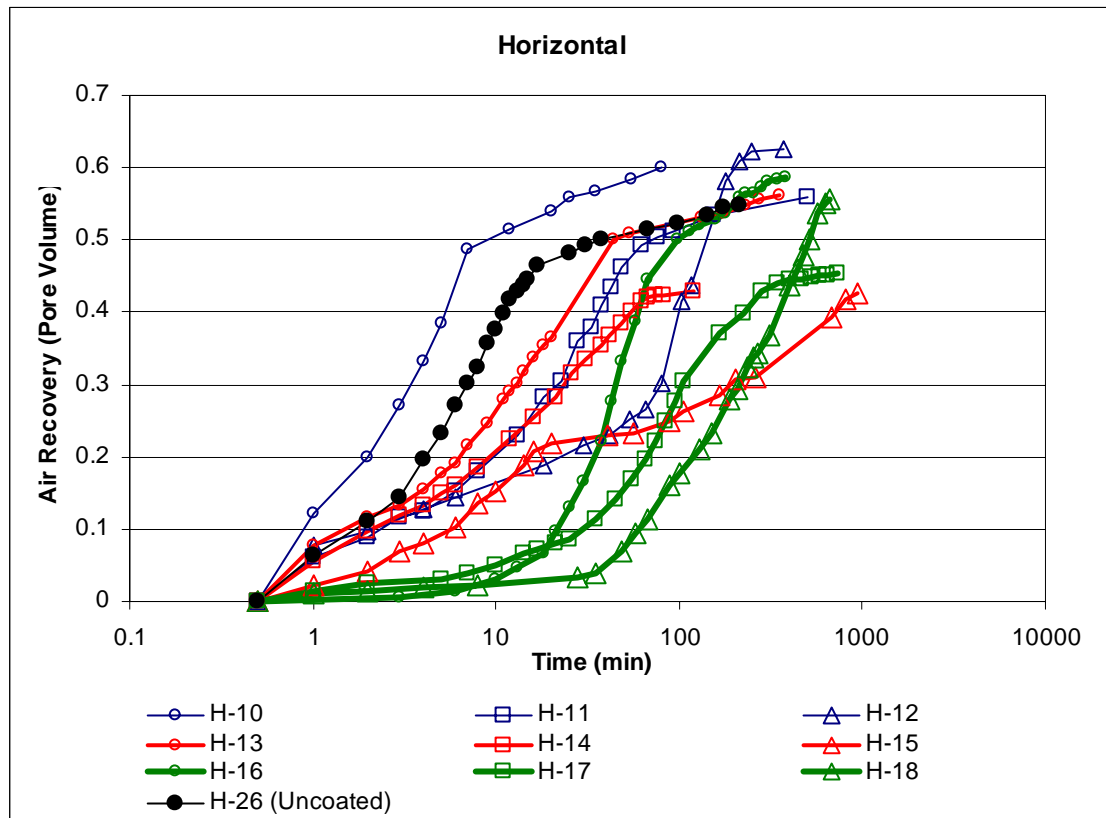


Figure 5: Air recovery by capillary imbibition of water from different matrix sizes and shapes for horizontally positioned samples at  $T=90^{\circ}\text{C}$ .

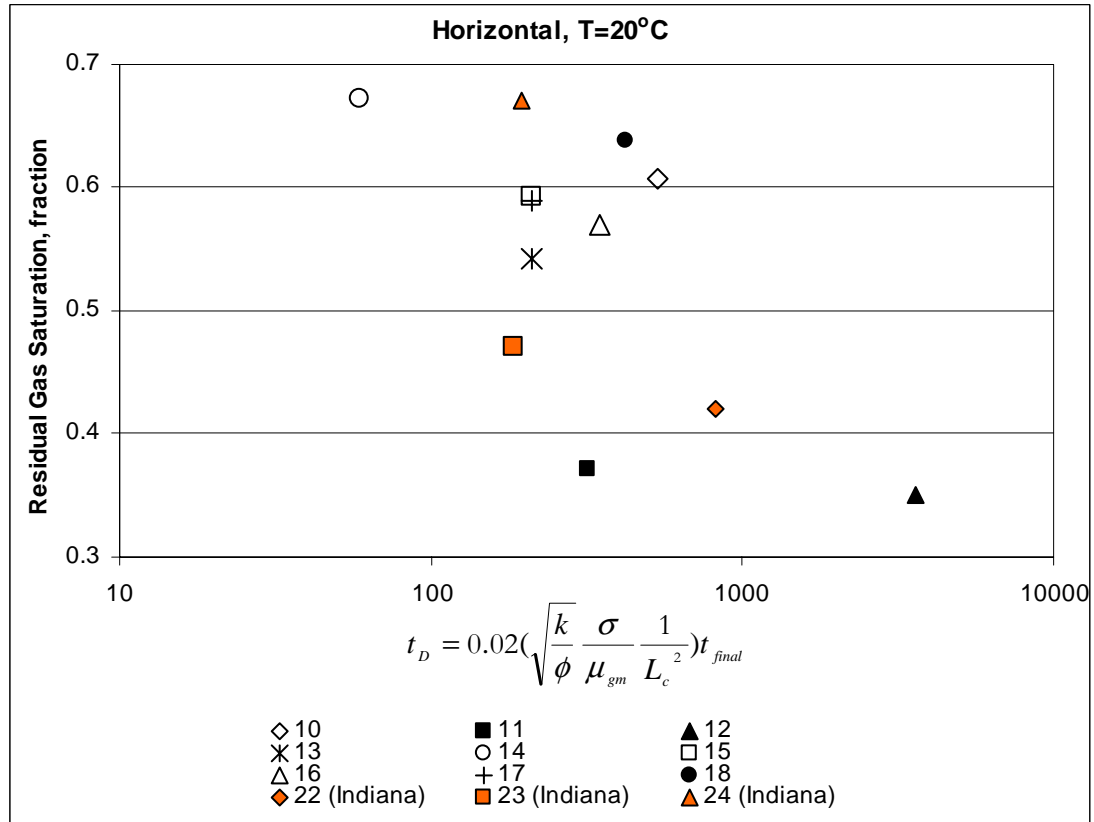


Figure 6: The change of residual gas saturation with the dimensionless group for horizontally positioned samples at  $T=20^{\circ}\text{C}$ .

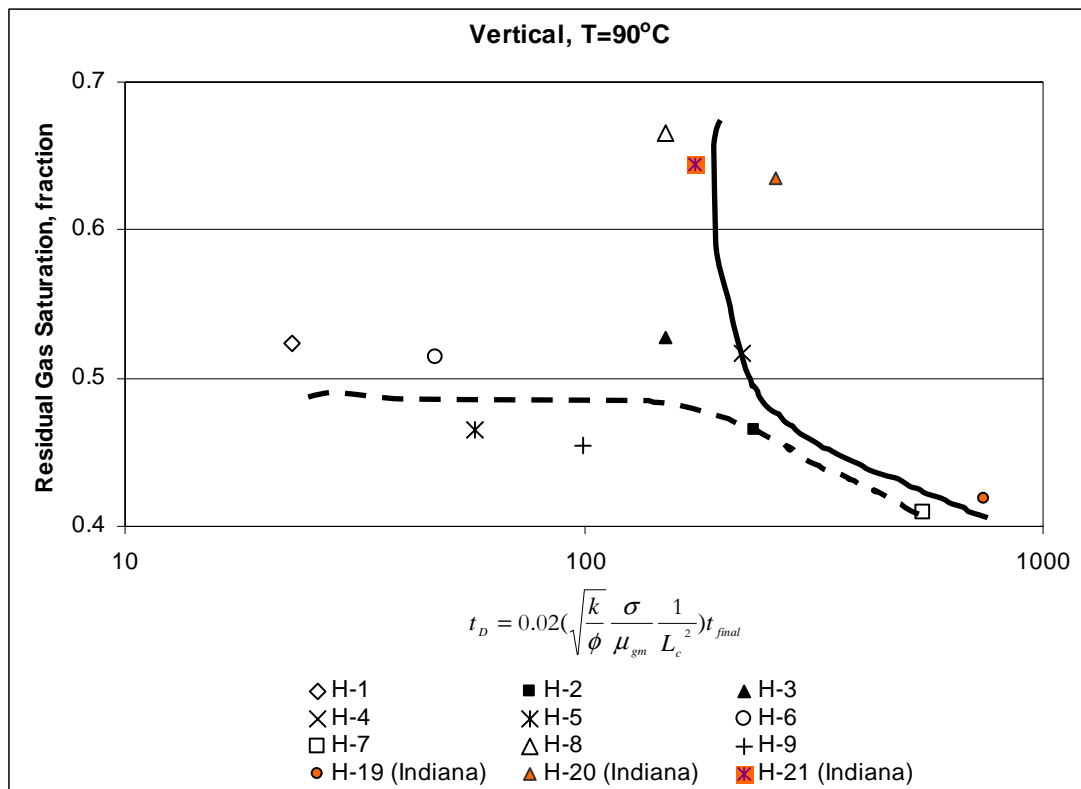


Figure 7: The change of residual gas saturation with the dimensionless group for vertically positioned samples at T=90°C.